Available online at www.sciencedirect.com
SCIENCE DIRECT®
ELSEVIER
Organic Electronics 4 (2003) 1–8
Organic Electronics
www.elsevier.com/locate/orgel

Volterra series analysis of the photocurrent in an Al/6T/ITO photovoltaic device

N. Boutabba *, L. Hassine *, N. Loussaief, F. Kouki, H. Bouchriha

LPMC, Faculté des Sciences de Tunis, Campus Universitaire, 1060 Tunis, Tunisia

Received 7 January 2002; received in revised form 10 August 2002; accepted 10 August 2002

Abstract

Using Volterra series we resolve analytically the non-linear rate equations describing the time evolution of the charge carrier concentration in an Al/6T/ITO cell when the device is illuminated and charge carriers are uniformally generated in the bulk at a known rate. We present the analytic expressions of the charge carrier densities in the bulk as a function of time and the expression for the photocurrent across the device. We show that the response contains a transient part and a permanent one. Using the first and the second order permanent response the photocurrent action spectrum of the device is obtained. We use these analytic results to suggest a method to evaluate experimentally the carrier lifetimes τ_n and τ_p and the Langevin bimolecular recombination rate. The system of rate equations has also been resolved numerically, using the Runge–Kutta method. Finally we compare successfully the measured photocurrent action spectrum with those obtained numerically and analytically.

Keywords: Volterra series; Photovoltaics; Al/6T/ITO; Photocurrent

1. Introduction

Sexithiophene (6T) is at present one of the most widely used model molecules of conjugated polymers [1,2]. One of its major advantages is the availability of single crystals, where the number of structural defects is much lower than in polymers or polycrystalline films. Conjugated polymers have been investigated for many years as the photoactive components in optoelectronic devices [3,4]. However, there is no clear theoretical description of optical and electronic phenomena in these materials. Theoretical models which successfully describe the photovoltaic action spectra of inorganic semiconductors could not be applied to conjugated polymers because the charge transport and semiconducting properties of these materials depend on the morphology of the polymer chain folding and arrangement and on photogeneration mechanisms with intricate competitive effects like the presence of traps and excitation states. In the field of polymers many models and analyses are based on the evolution equations of the electron and hole population densities. Overall system behaviour could be predicted using proper analytical techniques; that is why analytical expressions give powerful tools for analysis and are necessary in the

* Corresponding authors.
E-mail addresses: n_boutabba@yahoo.fr (N. Boutabba), lotfi.hassine@fst.rnu.tn (L. Hassine).

1566-1199/02/$ - see front matter
doi:10.1016/S1566-1199(02)00065-4

determination of the performance of a system. We use here a method that can be applied to every non-linear system of differential equations [5]. It makes it possible to interpret *analytically* some experimental results which are otherwise difficult to analyse. In the present paper we resolve the rate equations describing the time evolution of the carrier concentrations in the device. Our purpose is to give an analytical expression of the photocurrent across an illuminated Al/6T/ITO [1] cell. First we describe the time evolution of the charge carriers in an Al/6T/ITO structure, operating as a photovoltaic cell. Second we present the Volterra and the power expansion series which allows to compute symbolically the response of the non-linear system considered here. Then, using these mathematical tools, we calculate analytically the response in terms of charge carrier concentrations and photocurrent as a function of time. We resolve numerically our kinetic system using the fourth order Runge–Kutta method. Finally we compare our theoretical results with the experimental ones.

2. The Al/6T/ITO photovoltaic cell

6T preparation and purification are described in [6,7]. 6T is sandwiched, by an evaporation process, between two asymetric electrodes: indium–tin–oxide (ITO) and aluminium (Al). The absorption spectrum of 6T thin films was obtained using a Cary 2300 spectrophotometer working in the visible range. The photocurrent action spectra were measured by intermittently illuminating the cell through the Al electrode with a tungsten halogen lamp (36 V, 400 W), at the entrance side of the monochromator and lock-in detection amplifier (ATNE). The frequency of the incident chopped light was chosen in such a way that the permanent regime was established for every single cycle (about tens of ms) [8]. The entire setup assembly was controlled by the software Keithley Das 1600.

Several studies of the mechanism of photogeneration of charge carriers in Al/6T/ITO cells have been reported [9,10]. Ghosh et al. [9] have shown that photoexcitation with a photon energy equal or larger than the energy gap of the device generates electron–holes pair in a narrow photoactive region, the depletion layer, which leads to free charge carriers in the bulk. They have also shown that the most photosensitive region is the interface between the aluminium and the 6T, and that the photocurrent depends on the ability of the minority carriers (electrons) to reach this interface which acts as a sink for them. In this work, interactions between carriers of the same type (electron–electron and hole–hole) are ignored because it is assumed, based on the Drude model, that in fact these interactions lead mainly to a damping effect. We note that an ohmic contact on a semiconductor is usually defined as a contact whose impedance is negligible compared to the total impedance of the device, and which does not affect the bulk carrier concentration far into the semiconductor [11]. Phenomenologically, the temporal variation of the free carrier concentration in the bulk is equal to the photogeneration rate minus the spontaneous recombination rate (the rate at which carriers are destroyed inside the bulk through the carrier lifetimes) and the bimolecular recombination losses. Then, if we denote the density of the holes by p and that of the electrons by n, the rate equations describing the time evolution of the concentration of carriers in the device when illuminated by a flux density of photons $\phi(t,x)$ are (c.f. [8])

$$\begin{aligned} \frac{\mathrm{d}n}{\mathrm{d}t} &= \alpha\phi(t,x) - \frac{n}{\tau_n} - Rnp, \\ \frac{\mathrm{d}p}{\mathrm{d}t} &= \alpha\phi(t,x) - \frac{p}{\tau_p} - Rnp, \end{aligned} \tag{1}$$

where τ_n and τ_p are the carrier life time of n and p, respectively, and a quantum yield of one has been assumed. The factor R denotes the bimolecular recombination rate, α is the absorption coefficient (cm^{-1}), ϕ is the incident photon flux density ($\mathrm{cm}^{-2}\,\mathrm{s}^{-1}$) considered as the input of our system. In Fig. 1 we show the experimental absorption spectrum. Since our sample (Al/6T/ITO) has a small thickness (150 nm) (Fig. 2), we can assume that the illumination is homogeneous through the

[1] ITO = indium–tin–oxide conductive semitransparent layer on a glass substrate.

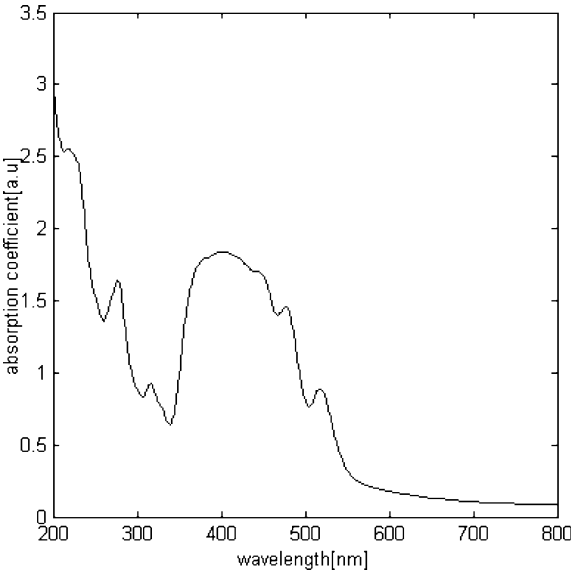

Fig. 1. The experimental absorption spectrum of 6T.

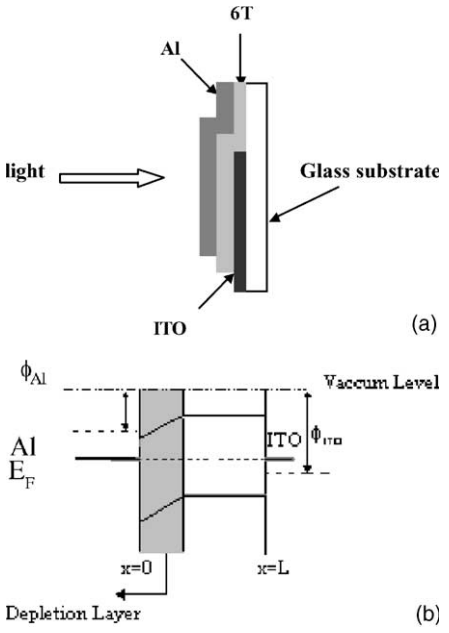

Fig. 2. Schematic view of an AL/6T/ITO cell and sketch of the energy band diagram.

device, consequently the generation term $\alpha\phi(t,x)$ becomes independent of x, i.e. $\phi(t,x) = \phi(t)$. Furthermore, in the nearly constant field assumption and with the absence of injected current, the density of the photogenerated carriers (e–h) is considered to be uniform $(\partial p/\partial x = \partial n/\partial x \simeq 0)$. For this reason, we do not consider the contributions of any divergence of either current described by (1); in fact we assume $\partial j_n/\partial x = \partial/\partial x[e\mu_n(nE + (kT/e)\partial n/\partial x)] \simeq 0$. Then the spatial dependencies in the equations are removed:

$$\begin{aligned} \frac{\mathrm{d}n}{\mathrm{d}t} &= \alpha\phi(t) - \frac{n}{\tau_n} - Rnp, \\ \frac{\mathrm{d}p}{\mathrm{d}t} &= \alpha\phi(t) - \frac{p}{\tau_p} - Rnp. \end{aligned} \tag{2}$$

3. Mathematical analysis

The Volterra series are defined by [12]

$$y(t) = h_0(t) + \int_0^t h_1(t,\tau_1)u(\tau_1)\,\mathrm{d}\tau_1 + \cdots + \int_0^t \int_0^{\tau_n} \cdots \int_0^{\tau_2} h_n(t,\tau_n \ldots \tau_1) \prod_{i=1}^{n} u(\tau_i)\,\mathrm{d}\tau_i, \tag{3}$$

where $y(t)$ is the system output and $u(t)$ is the system input assumed, for simplicity, to be scalar; h_n is the nth order Volterra kernel. Although the Volterra series has been successfully used in many applications, it has not received a great deal of attention. The reason seems to be that tedious computations are involved in the determination of Volterra kernels. Moreover, it is often difficult to obtain the response for a given input, even when the Volterra kernels are known. To overcome this difficulty and to resolve symbolically the nonlinear system, we associate to each basic variable (n and p in our case), a new symbolic variable g called generating power series (GPS), which represents the Laplace–Borel transforms of n and p. The expression in the time domain of (3) is represented by the following formal generating power series called GPS [13,14]:

$$g = \sum_{n \geqslant 0} \sum_{i_0,i_1,\ldots,i_n \geqslant 0} h_n^{(i_0,i_1,\ldots,i_n \geqslant 0)} z_0^{i_n} z_1 \cdots z_0^{i_1} z_1 z_0^{i_0}. \tag{4}$$

Moreover, the GPS can be obtained directly from the kinetic system (2), and using some algebraic rules, we calculate g_n and g_p. The latter lead to n

and p by taking the inverse Laplace–Borel transform.

As shown in Appendix A, the mathematical model is a powerful tool allowing for a complete treatment and giving full analytic solutions for non-linear systems. The complete solution of the coupled equations (2) in second order is given by

$$\begin{aligned} p = {} & a\tau_p\left(1-\mathrm{e}^{\frac{-t}{\tau_p}}\right)+a^2R\frac{(\tau_n\tau_p)^2}{(\tau_n+\tau_p)} \\ & \times\left(1-\frac{(\tau_n+\tau_p)\mathrm{e}^{\frac{-t}{\tau_p}}}{(\tau_p-\tau_n)}-\mathrm{e}^{\frac{-(\tau_n+\tau_p)t}{\tau_n\tau_p}}-\frac{(\tau_n+\tau_p)\mathrm{e}^{\frac{-t}{\tau_n}}}{(\tau_n-\tau_p)}\right) \\ & +a^2R\frac{\tau_n\tau_p^3}{(\tau_n+\tau_p)}\left(1-\frac{\tau_n^2}{\tau_p^2}\mathrm{e}^{\frac{-(\tau_n+\tau_p)t}{\tau_n\tau_p}}-\frac{(\tau_n+\tau_p)}{\tau_p}\right. \\ & \left.\times\left(1-\frac{\tau_n}{\tau_p}-\frac{t}{\tau_p}\right)\mathrm{e}^{\frac{-t}{\tau_p}}\right), \end{aligned} \tag{5}$$

$$\begin{aligned} n = {} & a\tau_n\left(1-\mathrm{e}^{\frac{-t}{\tau_n}}\right)+a^2R\frac{(\tau_n\tau_p)^2}{(\tau_n+\tau_p)} \\ & \times\left(1-\frac{(\tau_n+\tau_p)\mathrm{e}^{\frac{-t}{\tau_n}}}{(\tau_n-\tau_p)}-\mathrm{e}^{\frac{-(\tau_n+\tau_p)t}{\tau_n\tau_p}}-\frac{(\tau_n+\tau_p)\mathrm{e}^{\frac{-t}{\tau_p}}}{(\tau_p-\tau_n)}\right) \\ & +a^2R\frac{\tau_p\tau_n^3}{(\tau_n+\tau_p)}\left(1-\frac{\tau_p^2}{\tau_n^2}\mathrm{e}^{\frac{-(\tau_n+\tau_p)t}{\tau_n\tau_p}}-\frac{(\tau_n+\tau_p)}{\tau_n}\right. \\ & \left.\times\left(1.-\frac{\tau_p}{\tau_n}-\frac{t}{\tau_n}\right)\mathrm{e}^{\frac{-t}{\tau_n}}\right). \end{aligned} \tag{6}$$

$p(t)$, $n(t)$ are the responses, describing the hole and electron population densities, respectively. The obtained solution contains two components: a permanent one and a transient one which consists of terms multiplied by $\exp(-t/\tau_p)$ or $\exp(-t/\tau_n)$. Moreover, we can clearly distinguish in the complete solution the first order response and the second order one (terms multiplied by αa^2). For instance the following expressions $p = a\tau_p(1-\mathrm{e}^{-t/\tau_p})$ and $n = a\tau_n(1-\mathrm{e}^{-t/\tau_n})$, correspond to the first order response. Note that the solutions are well-defined. In fact, as is known, the response of a non-linear system using the Volterra series is the sum of elementary responses $y_i(t)$ (Fig. 3); each term corresponds to the ith order of the system defined by it's Volterra kernel $h_i(t,\tau_i,\ldots,\tau_1)$. The first order part of our system is described by

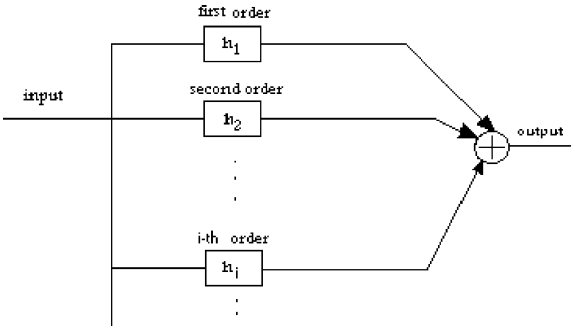

Fig. 3. Schematic view of a non-linear system decomposed according to the Volterra approach.

$$\begin{aligned} \frac{\mathrm{d}n}{\mathrm{d}t} &= \alpha\phi(t)-\frac{n}{\tau_n}, \\ \frac{\mathrm{d}p}{\mathrm{d}t} &= \alpha\phi(t)-\frac{p}{\tau_p}. \end{aligned} \tag{7}$$

One can easily resolve this system with zero time initial conditions and $\phi(t) = \phi_0 u(t)$ to obtain the same results as given by the first order response of (5) and (6). According to the definition of the Volterra kernel [15], we give the expressions of the first and the second order Volterra kernel of n as

$$\begin{aligned} h_1(t) &= \tau_n\mathrm{e}^{-t/\tau_n}u(t), \\ h_2(t_1,t_2) &= R\tau_p\left(\mathrm{e}^{\frac{-t_2}{\tau_n}}-\mathrm{e}^{-t_2\left(\frac{1}{\tau_n}+\frac{1}{\tau_p}\right)}\right)(\mathrm{e}^{-t_1/\tau_n}+\mathrm{e}^{-t_1/\tau_p}). \end{aligned} \tag{8}$$

To obtain the Volterra kernel of p we replace τ_p by τ_n and τ_n by τ_p.

For $t\to\infty$, the second order expressions of the hole and of the electron density become

$$\begin{aligned} p &= a\tau_p+\frac{(\tau_n\tau_p)^2}{(\tau_n+\tau_p)}a^2R+\frac{\tau_n\tau_p^3}{(\tau_n+\tau_p)}a^2R, \\ n &= a\tau_n+\frac{(\tau_n\tau_p)^2}{(\tau_n+\tau_p)}a^2R+\frac{\tau_p\tau_n^3}{(\tau_n+\tau_p)}a^2R. \end{aligned} \tag{9}$$

These new expressions correspond to the steady-state regime.

4. Discussion

In Figs. 4 and 5 we present the analytical responses which correspond to the time evolution of

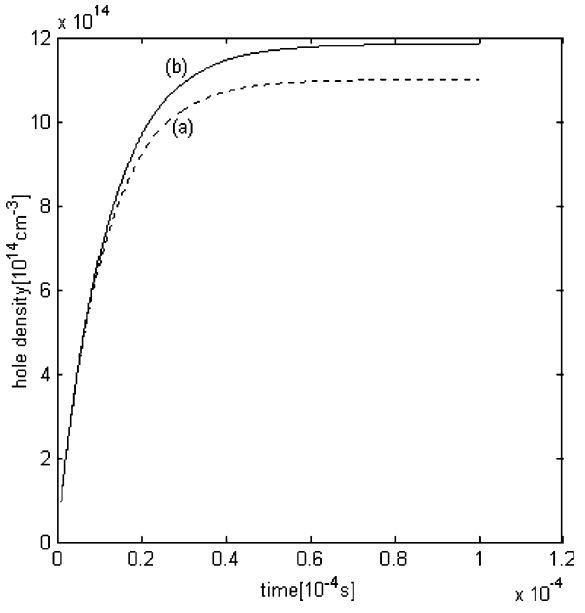

Fig. 4. Calculated electron density as a function of time: (a) first order, (b) complete solution (first and second order).

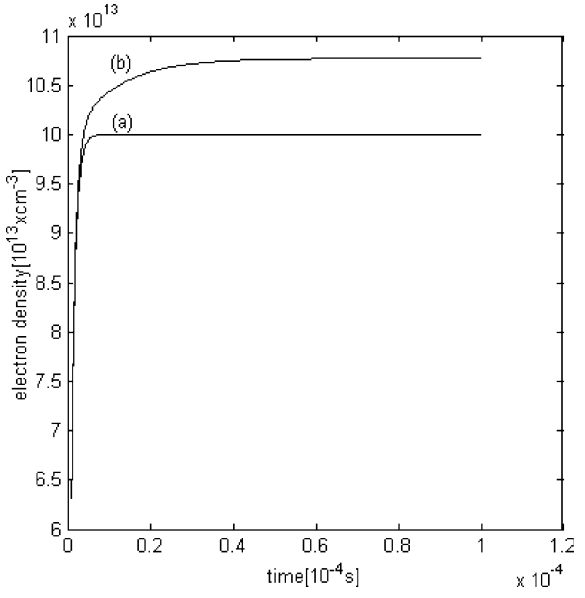

Fig. 5. Calculated hole density as a function of time: (a) first order, (b) complete solution (first and second order).

the electron and hole density, in the crystal. We show a transient and a permanent behaviour, in fact the densities increase with time and become constant after a few microseconds. This time is less than the experimental illumination period which implies that the permanent regime is reached for each cycle. If we compare the carrier density in the first order with that of the second order we find that $\Delta n/n \simeq \Delta p/p \simeq 8\%$. Thus the second order contribution is not negligible.

The photocurrent across the Al/6T/ITO cell is proportional to the charge carrier density as

$$I = e\mu_n ESn + e\mu_p ESp, \tag{10}$$

where e is the elementary charge, μ the mobility of the carriers estimated as $\mu_n = 1.5 \times 10^{-4}$ cm^2/V s and $\mu_p = 1.5 \times 10^{-5}$ cm^2/V s [8], S the cross-section of the device ($S \simeq 1$ mm^2), and E the electric field in the depletion layer. To evaluate E we can consider the work functions of Al and ITO as 4.2 and 4.8 eV respectively; the width of the depletion layer is assumed to be about 12×10^{-6} cm [8]. Then we find $E \simeq 10^4$ V cm^{-1} which seems to be a realistic value. To evaluate the recombination rate constant, we consider that the dielectric constant of the organic materials used is always small (typically $\varepsilon \sim 3$–4), so Coulomb screening is inefficient and the distance $r_c = e^2/4\pi\varepsilon\varepsilon_0 k_B T$ at which the attractive interaction between an electron and a hole is $\geqslant k_B T$, is large, typically 15 nm at room temperature. The capture then results from a process of diffusion in a field, as in the case of weakly ionized dense gases treated long ago by Langevin. Hence the large capture cross-sections can be estimated as $\pi r_c^2 \sim 10^{-11}$ cm^2, and the large recombination rate constant obeys the following relation [16]:

$$R = \frac{e(\mu_n + \mu_p)}{\varepsilon\varepsilon_0}, \tag{11}$$

where ε_0 is the vacuum permittivity ($\varepsilon_0 \sim 8.85 \times 10^{-12}$ F m^{-1}). We obtain $R \sim 7 \times 10^{-12}$ cm^3 s^{-1}. These numerical values are used to compute the analytic current response.

Using the Runge–Kutta method, the differential equation system (2) is resolved numerically to obtain the carrier densities n and p as a function of time. Based on the permanent solutions and with the relation (10) we deduce the numerical photocurrent action spectrum.

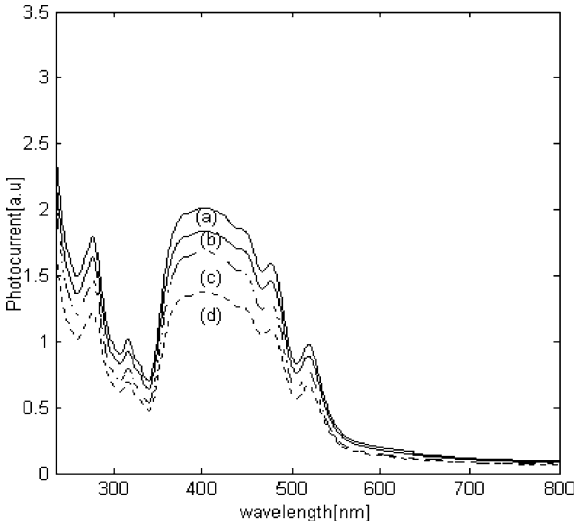

Fig. 6. Photocurrent action spectrum: (a) numerical spectrum, (b) measured spectrum, (c) calculated spectrum with first and second order contribution, (d) calculated first order spectrum.

In Fig. 6 we present the experimental (b) as well as the numerically (a) and the analytically (c, d) calculated photocurrent action spectra when the device is illuminated by a flux density of light $(\phi(t,x) = \phi_0 u(t))$ from an echelon grating. Each spectrum shows a more or less intense hump for $\lambda \leqslant 560$ nm and decreases sharply for larger wavelengths. As expected, we can see that the complete solution (up to the second order) is in better agreement with the experimental action spectrum than the first order approximation. There is also a good agreement between the numerical and the experimental curves.

We wish to suggest a method to evaluate experimentally the lifetimes τ_n, τ_p and R; we begin by writing the rate equations (2) as

$$\begin{aligned} \frac{dn}{dt} &= \alpha\phi(t) - \frac{n}{\tau_n^*}, \\ \frac{dp}{dt} &= \alpha\phi(t) - \frac{p}{\tau_p^*}, \end{aligned} \tag{12}$$

where $1/\tau_n^* = 1/\tau_n + Rp$ and $1/\tau_p^* = 1/\tau_p + Rn$ are the effective lifetimes of the carriers. Fig. 7 shows these lifetimes as functions of the incident flux density. If we can evaluate experimentally τ_n^* and τ_p^*, we can deduce the experimental values of τ_n and τ_p that correspond to τ_n^* and τ_p^* at $\phi = 0$, respectively. The bimolecular recombination rate R can also be evaluated as the slope of the derivative of τ_n^* or τ_p^* with respect to ϕ.

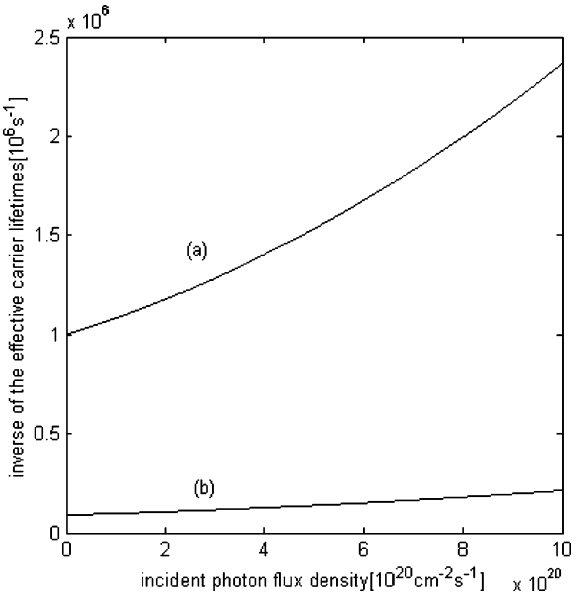

Fig. 7. Dependence of the inverse of the carrier effective lifetimes on the incident photon flux density: (a) $1/\tau_n^*$, (b) $1/\tau_p^*$.

5. Conclusion

In this work, using the Volterra series analysis we have resolved a set of non-linear differential equations describing the dynamical behaviour of carriers in an Al/6T/ITO photovoltaic cell for a space- and time-independent generation rate. The Volterra series analysis allows us to study non-linearities of the device. The obtained results are given analytically in their complete form. Thanks to this method, we found theoretical expressions of the hole and electron densities and of the photocurrent action spectra. We have shown that the contribution of the second order is not negligible, contrary to what has been assumed frequently. The theoretical photocurrent action spectra of the first and second order are computed; these compare well with the experimental ones. The presence of an absorption band between 350 and 500 nm leading to free charge carriers corresponds to the spectral range, where the device can be used as an

organic photodiode. Theoretical models are necessary in the design and optimization of non-linear systems, for example the Volterra kernels obtained here could be implemented in CAD developements to evaluate easily the photovoltaic performance for a given device. We plan to continue investigating more samples and to look for an experimental method to measure the effective charge carrier lifetimes, to be able to deduce the bimolecular Langevin recombination rate and the microscopic lifetimes of the charge carriers.

Appendix A

Several physical systems, for example a photovoltaic cell, can be described by the following typical coupled differential equations:

$$\begin{aligned}\dot{x}_1 &= \lambda_1 x_1 + a^1_{20}x_1^2 + a^1_{02}x_2^2 + a^1_{11}x_1x_2 + a\phi(t),\\ \dot{x}_2 &= \lambda_2 x_2 + a^2_{20}x_1^2 + a^2_{02}x_2^2 + a^2_{11}x_1x_2 + a'\phi(t),\end{aligned} \tag{A.1}$$

where $\phi(t)$ is the input and $x_1(t)$ and $x_2(t)$ are the outputs. Brockett [17] has shown, using the Carleman linearisation method, that a set of bilinear systems can be associated with a non-linear one where the nth derived bilinear system has the same n first Volterra kernels as the ones found in the non-linear system. Let us consider the following non-linear system and assume that the 0th order Volterra kernel is zero. $\phi(t)$ is the input of our system and $x_1(0) = x_2(0) = 0$ are the initial conditions. We introduce a set of variables:

$$x_{ij} = x_1^i x_2^j. \tag{A.2}$$

By differentiating Eq. (A.2) we obtain

$$\dot{x}_{ij} = i\dot{x}_1 x_1^{i-1}x_2^j + jx_1^i\dot{x}_2x_2^{j-1}. \tag{A.3}$$

By inserting (A.1) in (A.3) and by eliminating the monomials for $i + j > n$ because these have no effect in the Volterra approximation of order n, we obtain, in the algebraic domain, the system of the GPS g^n_{ij} [15] associated with $x_{ij}(t)$; then we deduce the g^2_{10}, and g^2_{01} associated with the variables $x_1 = p$, $x_2 = n$.

The g^n_{ij} (of order n), are given by

if

$i + j = n$,

$$g^n_{ij} = (1 - (i\lambda_1 + j\lambda_2)z_0)^{-1}\left(iaz_1g^{n-1}_{(i-1)j} + ja'z_1g^{n-1}_{i(j-1)}\right);$$

if

$i + j \leqslant n$,

$$\begin{aligned}g^n_{ij} = (1 - (i\lambda_1 + j\lambda_2)z_0)^{-1}\Big((ia^1_{20} + ja^2_{11})z_0g^n_{(i+1)j}\\ + (ia^1_{11} + ja^2_{02})z_0g^n_{i(j+1)} + ia^1_{02}z_0g^n_{(i-1)(j+2)}\\ + ja^2_{20}z_0g^n_{(i+2)(j-1)} + iaz_1g^{n-1}_{(i-1)j} + ja'z_1g^{n-1}_{i(j-1)}\Big);\end{aligned} \tag{A.4}$$

where the letter z_0 corresponds to the integration [15] with respect to time and the letter z_1 denotes the integration with respect to time after multiplying by the input $\phi(t)$.

Note that this formal computing for non-linear systems generalizes the Heaviside calculus for linear systems. For the calculation we must compute first g^1_{10}, g^1_{01}, then g^2_{20}, g^2_{11}, g^2_{02}, g^2_{10}, g^2_{01}, and so on.

The GPS of our system up to second order are expressed by

$$\begin{aligned}g^2_{10} = a\left(1 + \frac{1}{\tau_p}z_0\right)^{-1}z_1 + a^2R\left(1 + \frac{1}{\tau_p}z_0\right)^{-1}\\ \times z_0\left(1 + \left(\frac{1}{\tau_p} + \frac{1}{\tau_n}\right)z_0\right)^{-1}z_1\left(1 + \frac{1}{\tau_n}z_0\right)^{-1}z_1\\ + a^2R\left(1 + \frac{1}{\tau_p}z_0\right)^{-1}z_0\left(1 + \left(\frac{1}{\tau_p} + \frac{1}{\tau_n}\right)z_0\right)^{-1}\\ \times z_1\left(1 + \frac{1}{\tau_p}z_0\right)^{-1}z_1,\end{aligned} \tag{A.5}$$

$$\begin{aligned}g^2_{01} = a\left(1 + \frac{1}{\tau_n}z_0\right)^{-1}z_1 + a^2R\left(1 + \frac{1}{\tau_n}z_0\right)^{-1}\\ \times z_0\left(1 + \left(\frac{1}{\tau_p} + \frac{1}{\tau_n}\right)z_0\right)^{-1}z_1\left(1 + \frac{1}{\tau_n}z_0\right)^{-1}z_1\\ + a^2R\left(1 + \frac{1}{\tau_n}z_0\right)^{-1}z_0\left(1 + \left(\frac{1}{\tau_p} + \frac{1}{\tau_n}\right)z_0\right)^{-1}\\ \times z_1\left(1 + \frac{1}{\tau_p}z_0\right)^{-1}z_1.\end{aligned} \tag{A.6}$$

For the step input, $\phi(t) = \phi_0u(t)$ where $u(t)$ is the Heaviside unit step function, we put $a = \alpha\phi_0$ and

we substitute the letter z_1 by the operator $z_0[g_\phi \otimes]$ in the expressions (A.5) and (A.6), where the symbol $\otimes$ designs the shuffle product which is a symbolic non-commutative rule [13], and g_ϕ represent the Laplace–Borel transform of the input $u(t)$ which is the identity. This leads to new expressions for g_{10}^2 and g_{01}^2 that depend only on z_0, which are finally expanded on partial-fraction terms. Our task in performing a partial-fraction expansion is to express g_{10}^2 and g_{01}^2 as a sum of simple fractions, then by taking the inverse Laplace–Borel transform of g_{10}^2 and g_{01}^2 we obtain the responses in the time domain (see (5) and (6)).

References

[1] G. Horowitz, F. Kouki, P. Valat, P. Delannoy, J. Roussel, Phys. Rev B. 59 (1999) 10651.
[2] J.H. Burroughes, D.D.C. Bradley, A.R. Brown, R.N. Marks, K. Mackey, R.H. Friend, P.L. Burns, A.B. Holmes, Nature 347 (1990) 539.
[3] I.D. Parker, R.W. Gymer, M.G. Harrison, R.H. Friend, H. Ahmed, Appl. Phys. Lett. 62 (1993) 1519.
[4] J.J.M. Halls, K. Pichler, R.H. Friend, S.C. Moratti, A.B. Holmes, Appl. Phys. Lett. 68 (1996) 3120.
[5] L. Hassine, Z. Toffano, F. Lamnabhi-Lagarrigue, A. Destrez, C. Birocheau, IEEE J Quant. Electron. 30 (1994) 918.
[6] P. Delonnoy, G. Horowitz, H. Bouchriha, F. Deloffre, J.L. Fave, F. Garnier, R. Hajlaoui, M. Heyman, F. Kouki, J.L. Monge, P. Valat, V. Wintgens, A. Yassar, Synth. Metals 67 (1994) 197.
[7] G. Horowitz, B. Bachet, A. Yassar, P. Lang, F. Demmanze, J.L. Fave, F. Garnier, Chem. Mater. 7 (1995) 1337.
[8] N. Loussaief, L. Hassine, N. Boutabba, F. Kouki, P. Spearman, F. Garnier, H. Bouchriha, Synth. Metals 128 (2002) 283.
[9] A.K. Ghosh, D.L. Morel, T. Feng, R.F. Show, C.A. Rowe Jr., J. Appl. Phys. 45 (1974) 230.
[10] K. Yamashita, N. Kihara, H. Shimidzu, H. Suzuki, Photochem. Photobiol. 35 (1982) 1.
[11] E.H. Rhoderick, R.H. Williams, Metal–Semiconductor Contacts, Oxford University Press, Oxford, 1988.
[12] M. Schetzen, The Volterra and Wiener Theories of Nonlinear Systems, Wiley, New York, 1980.
[13] M. Fliess, M. Lamnabhi, F. Lamnabhi-Lagarrigue, IEEE Trans. Circuits Sys. 30 (1983) 554.
[14] M. Lamnabhi, Sys. Contr. Lett. 2 (1982) 154.
[15] L. Hassine, Z. Toffano, F. Lamnabhi-Lagarrigue, A. Destrez, C. Birocheau, IEEE J Quant. Electron. 30 (1994) 918.
[16] M. Shott, C.R. Acad. Sci. Paris Appl. Phys. 1 (2000) 381.
[17] R.W. Brockett, Automatica 12 (1976) 167.